53rd AIAA Aerospace Sciences Meeting, January 5 - 9 2015, Kissimmee, FL

High-Order Moving Overlapping Grid Methodology for Aerospace Applications

Brandon Merrill,* Yulia Peet†

The development of a three dimensional spectrally accurate moving overlapping grid technique that is utilized to solve for the flow around complex moving geometries opens doors to various practical applications that have previously been difficult to model. This method provides a straightforward approach to managing grid resolution near moving structures without the need for mesh restructuring techniques. Building upon our previously validated overlapping mesh methodology, we have developed a moving overlapping mesh method in a high-order spectral element computational fluid dynamics solver. Current validation tests on the two dimensional moving overlapping grid methodology have shown spectral accuracy of the coupled solution for both translating and rotating meshes, and results for fluid interactions with translating structures that correlate well with experimental and other computational data. A three dimensional simulation demonstrates robustness of the method and the ability to represent flow around complex structures moving in complex ways, paving the way to accurately model the flow through a rotating wind turbine.

I. Introduction

The ability to flexibly and efficiently model the interaction of fluid with moving structures allows for analysis of numerous problems that have previously been very difficult to simulate. The motion of a three dimensional mesh able to move with six degrees of freedom (translational and rotational) envelops the possibility to model a wide range of useful applications spanning from the flow around helicopter blades, wind turbines, propellers, to flows in engines, mixed tanks, stirred reactors, and much more. The use of moving overlapping grids, especially when one or both of the grids contain solid bodies, enables a straightforward approach to managing grid resolution near walls without the need for grid restructuring techniques.

The earliest known technique in domain decomposition methods was developed by Schwarz in 1870 with the introduction of the Schwarz Alternating Method. Schwarz provided a foundation upon which almost all other domain decomposition methods are built. Additional fundamental work with overlapping grids was performed in the 1960's by Volkov[1] who called his technique the Composite Mesh Difference Method that used finite difference methods on overlapping two dimensional grids. Since that time, many others have built upon his work improving the Composite Mesh Difference Method.[2–4] This work in composite mesh methods led to the development of techniques like those produced by Henshaw et al.[5] Henshaw's work involves a moving overlapping grid technique in two dimensions which utilizes boundary fitted grids that move on an overlapped stationary background Cartesian grid where one grid determines data for adaptive mesh refinement. Their method uses a second order extension of Godunov's method with adaptive mesh refinement for spatial discretization. Another derivation of multigrid methods is employed by Rivera et al.[6] who has developed a sliding mesh technique for finite element simulations. Their technique utilizes three dimensional meshes that remain adjacent to each other, without overlap, and one mesh is constrained to move. When using this method for rotational motion, the rotating mesh must necessarily be circular. Additional research has been performed by many others using sliding mesh techniques to simulate three dimensional flows with complex geometries.[7–9] In addition, there has been much work done with respect

*PhD Candidate, School for Engineering of Matter, Transport, and Energy (SEMTE), Arizona State University; E-mail: brandon.merrill@asu.edu

†Assistant Professor, School for Engineering of Matter, Transport and Energy (SEMTE), Arizona State University

to moving objects on a single mesh using numerous methods including the Arbitrary Lagrangian-Eulerian method.[10–13] Our research will improve upon previous methods by using the Spectral Element Method on three dimensional meshes, which maintains spectral accuracy for spatial discretization, and by utilizing moving overlapping grid techniques with spectral interpolation for flexibility of motion, and computational efficiency.

Our research builds upon a domain decomposition technique employed within the computational fluid dynamics (CFD) code, Nek5000, developed at the Mathematics and Computer Science Division of Argonne National Laboratory.[14] The governing equations of incompressible fluid flow (the incompressible Navier-Stokes equations) will be expressed using the Eulerian formulation for stationary meshes, which requires the computational domain to be fixed in space, and for moving meshes, the Arbitrary Lagrangian-Eulerian formulation is used, which allows the velocity of the mesh to be *arbitrarily* specified. In all overlapping cases, the values at the subdomain interfaces are handled using spectral interpolation with an explicit extrapolation method.

Building upon our overlapping mesh methodology, work was done to enable the use of moving meshes. We used an Arbitrary Lagrangian-Eulerian formulation as a platform for handling non-stationarity of the mesh. We have also performed simulations to test the stability and validity of the code. Convecting eddy simulations were used to verify the spatial and temporal accuracy of the method. The capacity to accurately represent interaction of fluid with the moving bodies was investigated using simulations representing a two dimensional oscillating cylinder in uniform flow. Robustness and flexibility of the method, in preparation for modeling wind turbine flows, is demonstrated by a simulation of two rotating cylinders in a uniform flow field.

In this paper, we present the details and results of work done in the development and validation of our moving overlapping grid methodology. Section II will give an overview of the techniques and formulations used to develop the moving overlapping mesh methods. Section III presents the current work done in validating our moving overlapping mesh method and Section IV will conclude with a brief summary and an overview of intentions for future work.

II. Methods

Our moving overlapping mesh method is employed within the Nek5000 computational fluid dynamics framework[14] which utilizes the Spectral Element Method for spatial discretization, and allows for up to third order temporal discretization for solutions to the incompressible Navier-Stokes equations 1. It improves upon our *stationary* overlapping mesh methodology by allowing for rotation and/or translation of one of the grids.

$$\begin{gathered}\frac{\partial \mathbf{u}}{\partial t} + \mathbf{u}\cdot\nabla\mathbf{u} = -\nabla\mathbf{p} + \frac{\mathbf{1}}{\mathrm{Re}}\nabla^{\mathbf{2}}\mathbf{u} \\ \nabla\cdot\mathbf{u} = \mathbf{0}\end{gathered} \tag{1}$$

II.A. Handling Interfaces Between Meshes

Values at mesh interfaces are determined using spectral interpolation on values from previous timesteps. The location of a point on the interface of domain one (Ω^1) is found in terms of the local coordinates of the corresponding element in Ω^2 by treating it as an optimization problem and minimizing residuals with the Newton-Raphson method.[15] Explicit interface extrapolation (IEXT) is carried out using the values interpolated from data at previous timesteps, with up to third order extrapolation. The m^{th} order extrapolation operator is given in equation 2 with the coefficients γ_{pm} given in table 1.

$$E_m\left[u\right]^n = \sum_{p=1}^{m} \gamma_{pm} u^{n-p} \tag{2}$$

Stability of the extrapolation method has been examined using the one-dimensional unsteady diffusion equation on two overlapping domains with uniform point distribution. The grids overlapped to ensure the grid points in the two domains coincided. The stability for the extrapolation scheme in the study was confirmed analytically to be unconditionally stable for first order extrapolation with the backwards-differentiation scheme of first or second order. For higher orders, the stability is dependent upon the mesh overlap size and the number of extrapolation iterations.[16]

Table 1. **Coefficients for the EXTm schemes, m=1,2,3**[16]

	γ_{p1}	γ_{p2}	γ_{p3}
p=1	1	2	3
p=2		-1	-3
p=3			1

II.B. Arbitrary Lagrangian-Eulerian Formulation

The Arbitrary Lagrangian Eulerian (ALE) formulation attempts to combine the attractive properties of both the Lagrangian formulation, where the reference system is attached to 'particles' in the fluid, and Eulerian formulation, where the reference system is fixed in space. Its main advantage is the ability to assign an arbitrary velocity to the mesh. The velocity assigned to the mesh can be determined by some property of the flow, or it can be predetermined and its movement unaffected by the flow. The explanation and derivation of the ALE formulation below follows the general process given by Deville et al.[17]

The material derivative of a variable, f, given by

$$\frac{Df}{Dt} = \frac{\partial f}{\partial t} + \mathbf{u} \cdot \nabla f \tag{3}$$

where $\mathbf{u}(\mathbf{x}, t)$ is the velocity of the fluid in the Eulerian formulation, describes the time evolution of f attached to material points. If a mesh is given a velocity of $\mathbf{w}(\mathbf{x}, t)$ that is not equal to $\mathbf{u}(\mathbf{x}, t)$, a pseudo-material derivative can be given for the mesh, as if virtual particles were attached to the moving mesh, which we will call the ALE derivative

$$\frac{\delta f}{\delta t} = \frac{\partial f}{\partial t} + \mathbf{w} \cdot \nabla f \tag{4}$$

Note that if $\mathbf{w}(\mathbf{x}, t) = 0$ we recover the Eulerian description, or simply the partial time derivative, and if $\mathbf{w}(\mathbf{x}, t) = \mathbf{u}(\mathbf{x}, t)$ we arrive at the material derivative in the Lagrangian description. A relative velocity, $\mathbf{c}$ (sometimes called the convective velocity), can be defined with respect to the reference frame of the moving mesh

$$\mathbf{u} = \mathbf{c} + \mathbf{w}. \tag{5}$$

The relationship between the material and ALE time derivative can then be given as

$$\frac{Df}{Dt} = \frac{\delta f}{\delta t} + \mathbf{c} \cdot \nabla f \tag{6}$$

To account for mesh movement, the convective terms in the Navier-Stokes equations must be altered to reflect the new relative velocity, $\mathbf{c}$.[12] Since density is held constant for incompressible flow, the convective term of the mass conservation equation is zero, and therefore, there is no change in the continuity equation. The momentum conservation equation becomes

$$\frac{\delta \mathbf{u}}{\delta t} + \mathbf{c} \cdot \nabla \mathbf{u} = -\nabla \mathbf{p} + \frac{\mathbf{1}}{\mathrm{Re}} \nabla^{\mathbf{2}} \mathbf{u} \tag{7}$$

where $\mathbf{c}$ is defined in equation 5. Again, note that if mesh velocity $\mathbf{w}$ is equal to zero, the original Navier-Stokes equations 1 are recovered.

II.C. Communicating Updates

Building upon the ALE formulation and interpolation schemes developed previously, additions and modifications were made to allow the two methods to work together. In the original multimesh method, the spatial coordinates of each interface node are passed to the corresponding processors once at the beginning of a simulation. Since the coordinates are constantly changing in the moving mesh formulation, modifications were made so that the new coordinates are passed during each timestep. This allows the velocities to be correctly interpolated/extrapolated during movement of the mesh.

III. Results: Moving Overlapping Meshes

III.A. Walsh's Eddies

The first moving mesh benchmark models the convecting solution to Walsh's eddies[18] on two overlapping meshes, with the inside mesh either rotating or sliding. The initial conditions are given by the stream function in equation 8,

$$\psi(x, y) = -\frac{1}{5}\mathrm{Cos}[5x] + \frac{1}{4}\mathrm{Sin}[3x]\mathrm{Sin}[4y] - \frac{1}{5}\mathrm{Sin}[5y] + u_0 y - v_0 x \tag{8}$$

giving exact solutions for the velocities of the convecting eddies

$$\begin{aligned} u(x, y) &= e^{-25t\nu}(-\mathrm{Cos}[5y] + \mathrm{Cos}[4y]\mathrm{Sin}[3x]) + u_0 \\ v(x, y) &= e^{-25t\nu}(-\mathrm{Sin}[5x] - \frac{3}{4}\mathrm{Cos}[3x]\mathrm{Sin}[4y]) + v_0. \end{aligned} \tag{9}$$

This case was used to determine spatial and temporal accuracy and to ensure that the interpolation/extrapolation was carried out correctly for moving overlapping meshes without the presence of any solid objects. Note that although the mesh is moving, there are not any physical structures attached to it, so it may be considered *virtual* movement since the movement of the mesh should have no affect on the flow. The original mesh configurations (at t=0) are shown in figure 1. The exterior mesh contains a vacancy in the center that is covered by the interior mesh.

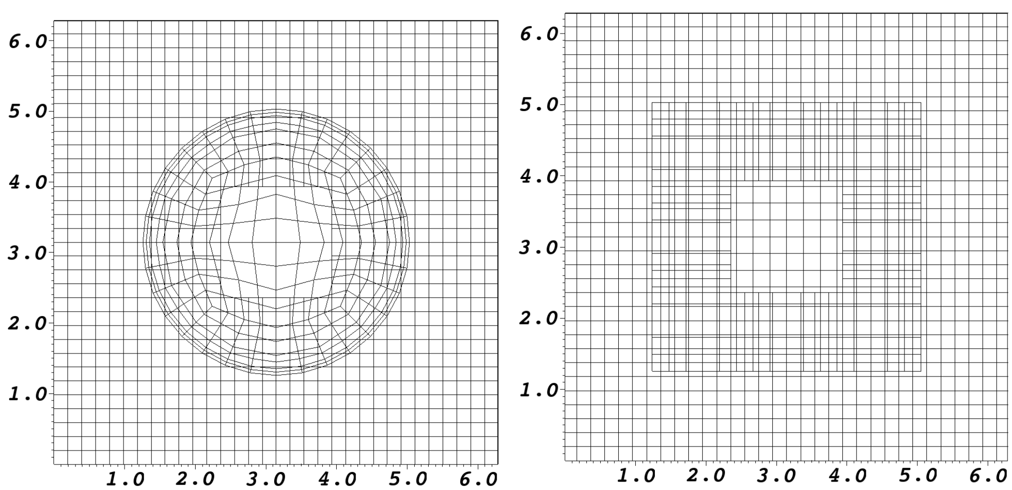

(a) Circular interior mesh (b) Square interior mesh

Figure 1. Two-mesh domains

The second order extrapolation scheme was used, and the angular velocity was fixed at $\frac{\pi}{4}$ for studying the spatial and temporal convergence of the method for the rotating cases. The velocity spatial convergence plots for both the square and circular rotating interior mesh simulations are shown in figure 2 with the non-rotating case results for comparison. The plots show spectral convergence and trends that correspond well to the stationary mesh data. The temporal accuracy, shown in figure 3 shows the expected second order convergence. Analysis of the pressure accuracy (not shown here) gives comparable results for both spatial and temporal convergence. The results from sliding mesh cases (not shown here) also show spectral accuracy for spatial discretization, and the expected second order temporal convergence. We see that the convergence rates of the underlying Spectral Element Method solver are maintained with the addition of our moving overlapping mesh method.

III.B. Oscillating 2D Cylinder in Uniform Flow

Since the earliest research performed by G Magnus[19] in 1852, a certain fascination has accompanied the research seeking to understand the flow around moving cylinders. The topic of oscillating or vibrating

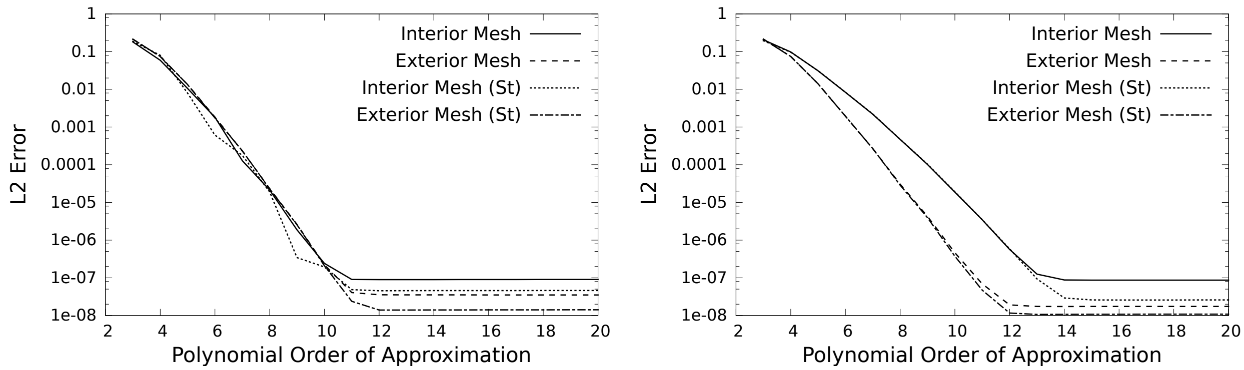

(a) Square interior mesh

(b) Circular interior mesh

Figure 2. Velocity spatial accuracy for rotating interior mesh simulations using second order time-stepping and EXT. 'St' indicates a stationary mesh case.

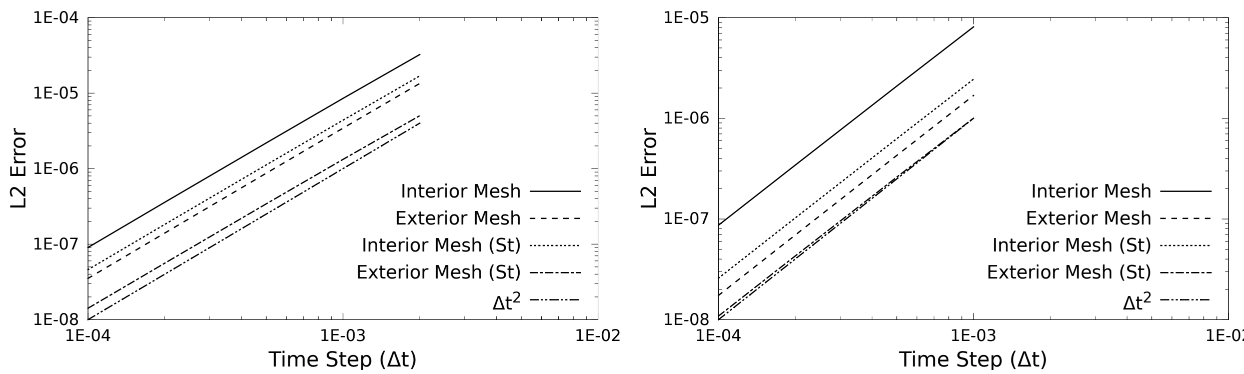

(a) Square interior mesh

(b) Circular interior mesh

Figure 3. Velocity temporal accuracy for rotating interior mesh simulations using a polynomial order of approximation of 18. 'St' indicates a stationary mesh case.

cylinders in cross-flow has been the subject of several experimental and computational studies.[20–24] In 1998, Blackburn et al. published results from an oscillating cylinder simulation that utilized a spectral elements code.[25] Their results, along with other published data, established detailed characteristics of the flow which allowed for comparison and validation of the present work.

For our oscillating cylinder simulations, the domain is assigned a uniform free stream velocity U at the left boundary with outflow conditions assigned on the opposing side. Symmetry boundary conditions are imposed on the top and bottom of the domain. Spatial units and the amplitude of the cylinder oscillation are non-dimensionalized by the diameter of the cylinder. The horizontal velocity of the cylinder is set to zero, while the vertical component of motion is governed by the equation

$$y(t) = y_0 + A\sin(2\pi f_0 t), \tag{10}$$

where A represents the amplitude and f_0 represents the frequency of oscillation. The cylinder is initially placed at (0,0), and the domain spans from $x = -10$ to 50 diameters, and from $y = -15$ to 15 diameters.

The exterior mesh (see fig. 4) contains a vacancy where the cylinder is placed, and the interior mesh was constructed around the 2D cylinder. During the simulations, the exterior mesh remained stationary while the prescribed motion of the interior mesh caused it to move with the equation of oscillation given by equation 10. The first task involved retrieving the Strouhal number from flow around the *stationary* cylinder. For a Reynolds number of 200, our simulations produced a Strouhal number of 0.1998 compared with the Strouhal number found in Udaykumar et al.[24] of 0.198 and the value found in Williamson et al.[23] of 0.197. The mean drag of our simulation was 1.372, while Udaykumar et al.[24] report a value of 1.38.

The drag and lift on an oscillating cylinder in a uniform cross-flow changes with time. However, after a sufficient startup time, the solution reaches an asymptotic state, indicated by values that repeat periodically

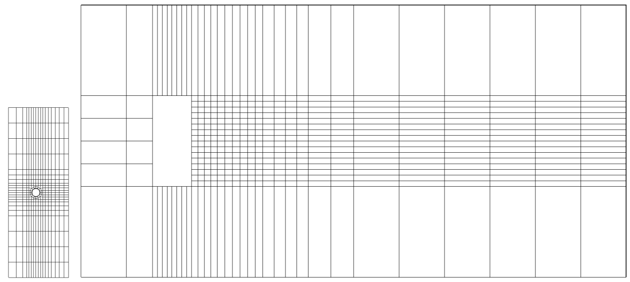

Figure 4. Geometry of the oscillating cylinder case

according to the motion of the cylinder. The results published in Blackburn et al.[25] include detailed information about the mean drag forces, the peak lift forces, and the mean pressure differences on the cylinder. Using the Strouhal number from stationary mesh simulations, the oscillation frequency of the cylinder is expressed as a ratio of the fixed-cylinder vortex shedding frequency. Table 2 compares the oscillating cylinder results with the results published by Blackburn et al.[25] for a frequency ratio of 1.0 and non-dimensional amplitude 0.25. The label $\widehat{C_l}$ represents the peak coefficient of lift, $\overline{C_d}$ is the mean coefficient of drag, and $\overline{C_{pb}}$ is the mean base pressure coefficient calculated from the pressures at the furthest upstream (p_0) and downstream (p_{180}) points on the cylinder surface, $C_{pb} = 1 + 2(p_{180} - p_0)/\rho U^2$.

	Blackburn et al.	Present Data
$\widehat{C_l}$	1.776	1.781
$\overline{C_d}$	1.414	1.417
$-\overline{C_{pb}}$	1.377	1.377

Table 2. Results for an oscillating cylinder with $Re = 500$, $F = 1$ and $A = 0.25$ in uniform flow compared with results from Blackburn et al.[25]

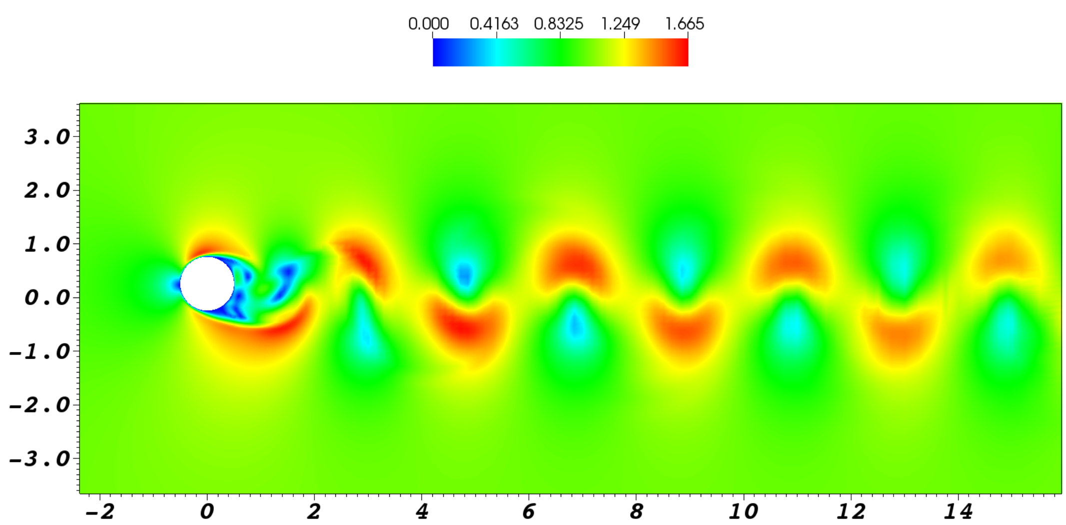

Figure 5. Zoomed-in velocity magnitude plot of a cylinder oscillating with properties: $A = 0.25$, $F = 1$, $Re = 500$

The velocity magnitude plot in figure 5 illustrates the vortices that are shed from an oscillating cylinder with a non-dimensional amplitude, $A = 0.25$ and a frequency ratio, $F = 1.0$, with a Reynolds number, $Re = 500$. The frequency of vortex shedding, the forces and pressure on the cylinder, and other flow characteristics correlate very well with available published data.

One primary benefit of our overlapping moving mesh method is the ability to model flows that are difficult or impossible to simulate using traditional methods, such as the flow around solid bodies moving with extreme ranges of motion. Figure 6 shows the velocity magnitude data from a case with a remarkably large amplitude ratio (A=2.5), much larger than any presently found published data. The overlapping moving mesh method gives accurate results for simulations containing solid bodies, and can simulate flows with extreme solid body motions that are impossible to model using traditional techniques.

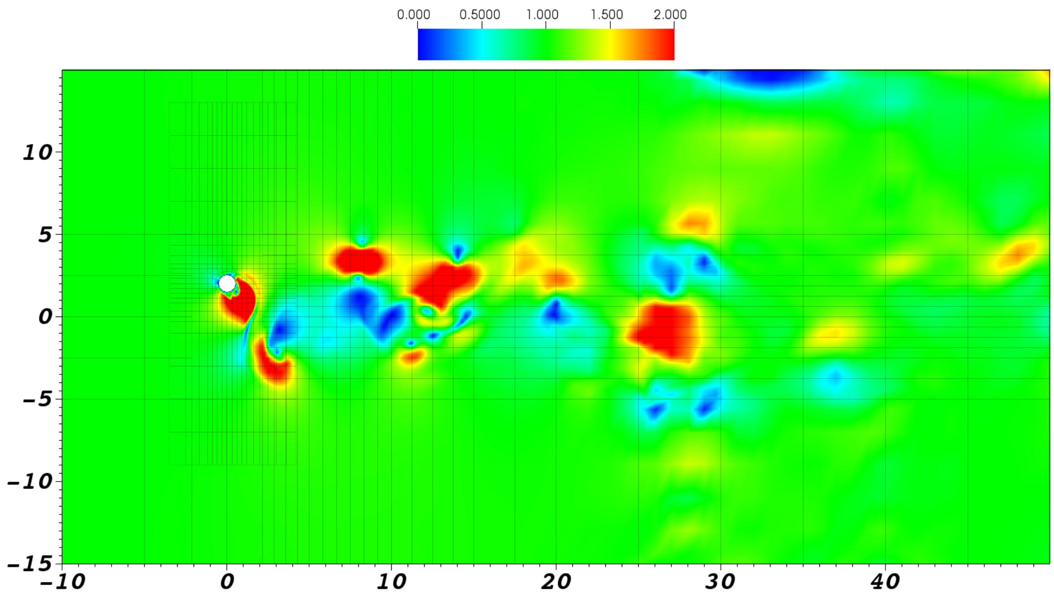

Figure 6. Velocity magnitude representation of the global domain for a cylinder oscillating with properties: $A = 2.5$, $F = 1$, $Re = 200$

III.C. Rotating 3D Cylinders

One of the benefits of an overlapping moving mesh method is the ability to accurately model fluid flow for cases involving a complex solid body geometry moving in a complex manner. One such situation is a horizontal axis wind turbine (HAWT). A future goal of the present project is to attain accurate data regarding the blade-wake, and wake-wake interactions in the flow through a rotating HAWT. To ensure that the method is adequately accurate and robust for these types of three dimensional rotational flows a preliminary test was performed using two cylinders exhibiting a similar motion to a rotating wind turbine.

The interior mesh, whose enlarged cross-section is shown in figure 7(a), was constructed around two 3-dimensional cylinders with diameter D, and the distance between the far ends of the two cylinders is 11D. The nearest node normal to the surface of the cylinders is approximately 0.03D away. The spatial resolution at the cylinder walls includes 10 elements in the span-wise direction of each cylinder and 16 elements radially around each cylinder. Note that the solution within each element is computed at several Gauss-Lobatto points, the number determined by the polynomial order of approximation established before the simulation is executed. The exterior mesh, a selection of which is shown in figure 7(b), contains a vacancy that is covered by the interior mesh . The global domain extends 30D upstream of the rotating cylinders and 50D downstream of the rotating cylinders, and the sides of the domain extend from -30D to 30D. The resolution of the interior mesh is much finer than that of the exterior mesh allowing greater ability to capture accurate solutions in the boundary layer.

Figure 8 depicts the vortices in the wake at the -0.05 λ_2 isosurface using second order extrapolation. The flow at the inlet of the domain is set to uniform velocity U, the tip speed ratio (TSR) of the rotating cylinders is 0.55, and the Reynolds number ($Re = \rho U D/\mu$) is 200. Realistic wind turbine flows have considerably larger Reynolds numbers, and thus in subsequent wind turbine simulations the mesh will be refined to adequately capture the small scale fluctuations, especially in the boundary layer region near the blade walls.

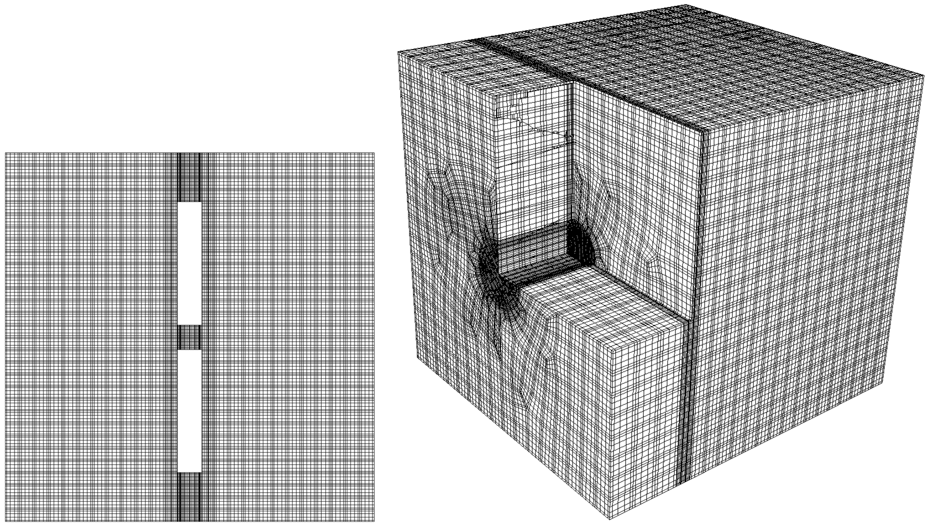

(a) Enlarged cross-section of the interior mesh

(b) Selection of exterior mesh

Figure 7. Geometry of rotating cylinders case

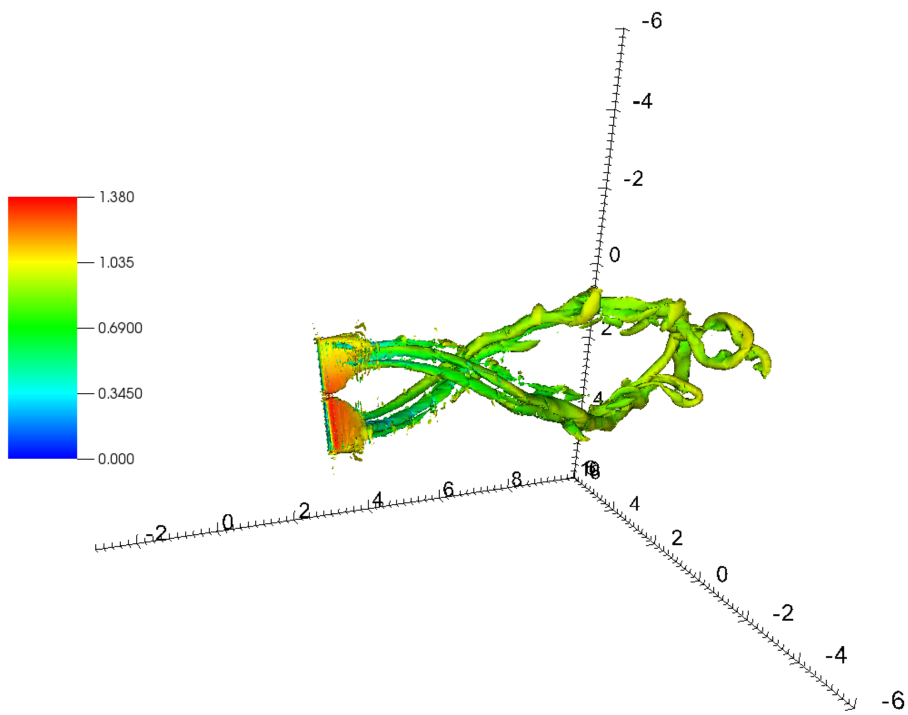

Figure 8. **λ_2 isosurfaces in the wake of two rotating cylinders with $TSR = 0.55$ and $Re = 200$**

IV. Conclusion

The validation benchmarks performed have shown good correlation with exact solutions where they are available, and with existing experimental and computational data. This new overlapping moving mesh method used with a Spectral Element Method solver opens doors to accurate flow simulations with moving geometries. Applications are endless and range from rotary wing aerodynamics, to oscillating pumps and pistons, to stirred reactors. The method will be used in the near future to study highly resolved wake structures and blade-wake interactions for a rotating wind-turbine rotor. Future development will allow the motion to be prescribed according to the forces on the structure, rather than prescribed by the user. Additional development must also be done to enable flow simulations around structures with both moving and stationary parts.

V. Acknowledgements

We would like to acknowledge support for this work given by the National Science Foundation grant CMMI-1250124.

References

[1]Volkov, E. A., "The method of composite meshes for finite and infinite regions with piecewise smooth boundary," *Trudy Matematicheskogo Instituta im. VA Steklova*, Vol. 96, 1968, pp. 117–148.

[2]Starius, G., "Composite mesh difference methods for elliptic boundary value problems," *Numerische Mathematik*, Vol. 28, No. 2, 1977, pp. 243–258.

[3]Starius, G., "On composite mesh difference methods for hyperbolic differential equations," *Numerische Mathematik*, Vol. 35, No. 3, 1980, pp. 241–255.

[4]Kreiss, B., "Construction of a curvilinear grid," *SIAM Journal on Scientific and Statistical Computing*, Vol. 4, No. 2, 1983, pp. 270–279.

[5]Henshaw, W. D. and Schwendeman, D. W., "Moving overlapping grids with adaptive mesh refinement for high-speed reactive and non-reactive flow," *Journal of Computational Physics*, Vol. 216, No. 2, 2006, pp. 744–779.

[6]Rivera, C. A., Heniche, M., Bertrand, F., Glowinski, R., and Tanguy, P. A., "A parallel finite element sliding mesh technique for the simulation of viscous flows in agitated tanks," *International Journal for Numerical Methods in Fluids*, Vol. 69, No. 3, 2012, pp. 653–670.

[7]Ng, K., Fentiman, N., Lee, K., and Yianneskis, M., "Assessment of sliding mesh CFD predictions and LDA measurements of the flow in a tank stirred by a Rushton impeller," *Chemical Engineering Research and Design*, Vol. 76, No. 6, 1998, pp. 737–747.

[8]Bakker, A., LaRoche, R. D., Wang, M.-H., and Calabrese, R. V., "Sliding mesh simulation of laminar flow in stirred reactors," *Chemical Engineering Research and Design*, Vol. 75, No. 1, 1997, pp. 42–44.

[9]Murthy, J., Mathur, S., and Choudhury, D., "CFD simulation of flows in stirred tank reactors using a sliding mesh technique," *Institution of Chemical Engineers Symposium Series*, Vol. 136, HEMSPHERE PUBLISHING CORPORATION, 1994, pp. 341–341.

[10]Hirt, C., Amsden, A. A., and Cook, J., "An arbitrary Lagrangian-Eulerian computing method for all flow speeds," *Journal of Computational Physics*, Vol. 14, No. 3, 1974, pp. 227–253.

[11]Donea, J., Giuliani, S., and Halleux, J., "An arbitrary Lagrangian-Eulerian finite element method for transient dynamic fluid-structure interactions," *Computer methods in applied mechanics and engineering*, Vol. 33, No. 1, 1982, pp. 689–723.

[12]Donea, J., Huerta, A., Ponthot, J.-P., and Rodríguez-Ferran, A., "Arbitrary lagrangian–eulerian methods," *Encyclopedia of computational mechanics*, 2004.

[13]Hu, H. H., Patankar, N. A., and Zhu, M., "Direct numerical simulations of fluid–solid systems using the arbitrary Lagrangian–Eulerian technique," *Journal of Computational Physics*, Vol. 169, No. 2, 2001, pp. 427–462.

[14]Fischer, P. F., Lottes, J. W., and Kerkemeier, S. G., "nek5000 Web page," 2008, http://nek5000.mcs.anl.gov.

[15]Peet, Y. and Fischer, P., "Heat Transfer LES Simulations in Application to Wire-Wrapped Fuel Pins," *Proceedings 10th AIAA/ASME Joint Thermophysics and Heat Transfer Conference*, 2010.

[16]Peet, Y. and Fischer, P. F., "Stability analysis of interface temporal discretization in grid overlapping methods," *SIAM Journal on Numerical Analysis*, Vol. 50, No. 6, 2012, pp. 3375–3401.

[17]Deville, M. O., Fischer, P. F., and Mund, E. H., *High-order methods for incompressible fluid flow*, Vol. 9, Cambridge University Press, 2002.

[18]Walsh, O., "Eddy solutions of the Navier-Stokes equations," *The Navier-Stokes Equations II - Theory and Numerical Methods*, Springer, 1992, pp. 306–309.

[19]Magnus, G., "On the Deflection of a Projectile," *Abhandlungen der Akademie der Wissenschaften, Berlin, Germany*, 1852.

[20]Bishop, R. and Hassan, A., "The lift and drag forces on a circular cylinder oscillating in a flowing fluid," *Proceedings of the Royal Society of London. Series A. Mathematical and Physical Sciences*, Vol. 277, No. 1368, 1964, pp. 51–75.

[21]Koopman, G., "The Vortex Wakes of Vibrating Cylinders at Low Reynolds Numbers," *Journal of Fluid Mechanics*, Vol. 28, No. 3, 1967, pp. 501–512.

[22]Williamson, C. and Roshko, A., "Vortex formation in the wake of an oscillating cylinder," *Journal of fluids and structures*, Vol. 2, No. 4, 1988, pp. 355–381.

[23]Williamson, C. H., "Vortex dynamics in the cylinder wake," *Annual review of fluid mechanics*, Vol. 28, No. 1, 1996, pp. 477–539.

[24]Udaykumar, H., Mittal, R., Rampunggoon, P., and Khanna, A., "A Sharp Interface Cartesian Grid Method for Simulating Flows with Complex Moving Boundaries," *Journal of Computational Physics*, Vol. 174, No. 1, 2001, pp. 345 – 380.

[25]Blackburn, H. and Henderson, R., "A study of two-dimensional flow past an oscillating cylinder," *Journal of Fluid Mechanics*, Vol. 385, 1999, pp. 255–286.